

Femtosecond holography in lithium niobate crystals

Hung-Te Hsieh and Demetri Psaltis

Department of Electrical Engineering, California Institute of Technology, Pasadena, California 91125

Oliver Beyer, Dominik Maxein, Clemens von Korff Schmising, and Karsten Buse

Institute of Physics, University of Bonn, Wegelerstrasse 8, D-53115 Bonn, Germany

Boris Sturman

Institute of Automation and Electrometry, 630090 Novosibirsk, Russia

Received March 24, 2005; accepted April 23, 2005

Spatial gratings are recorded holographically by two femtosecond pump pulses at 388 nm in lithium niobate (LiNbO₃) crystals and read out by a Bragg-matched, temporally delayed probe pulse at 776 nm. We claim, to our knowledge, the first holographic pump-probe experiments with subpicosecond temporal resolution for LiNbO₃. An instantaneous grating that is due mostly to the Kerr effect as well as a long-lasting grating that results mainly from the absorption caused by photoexcited carriers was observed. The Kerr coefficient of LiNbO₃ for our experimental conditions, i.e., pumped and probed at different wavelengths, was $\approx 1.0 \times 10^{-5}$ cm²/GW. © 2005 Optical Society of America
OCIS codes: 050.7330, 190.3270, 190.4380, 190.7110.

Ferroelectric lithium niobate (LiNbO₃) crystals are one of the most investigated materials for widespread and promising applications in nonlinear optics, e.g., for parametric amplification and second-harmonic generation.¹ LiNbO₃ also shows photorefractive properties,² which are characterized by a change in its refractive index that results from an optically induced separation of electrons and the linear electro-optic effect. The ability to record holograms makes LiNbO₃ crystals attractive for many applications such as holographic data storage, optical information processing, phase conjugation, and wavelength filters.^{3,4}

Pulses with temporal durations of tens of picoseconds and peak intensities of 0.1 to 1 GW/cm² were previously used to investigate the photorefractive effects in various materials, e.g., bismuth silicate (Bi₁₂SiO₂₀),⁵ barium titanate (BaTiO₃),⁶ and potassium niobate (KNbO₃).⁷ Femtosecond pulses were used for nonvolatile spectral holography in LiNbO₃,⁸ but pump-probe experiments that allow its ultrafast material response to be studied have not been conducted to our knowledge. In this Letter we investigate holograms recorded in LiNbO₃ with femtosecond pulses at 388 nm. Grating-recording experiments have been conducted extensively in LiNbO₃ at low intensities (≈ 1 W/cm²) with continuous-wave lasers and at high intensities (up to ≈ 10 MW/cm²) by nanosecond pulses.^{9,10} At these intensity levels, the photorefractive effect is still the dominant nonlinear effect; however, holographic recording with even more intense pulses will reveal other nonlinear material responses. The enhanced temporal resolution obtained with femtosecond pulses and accumulated knowledge about two-photon absorption^{11,12} enable us to draw conclusions about the participating nonlinear processes.

The experimental setup is illustrated in Fig. 1. Two pump pulses at $\lambda_p = 388$ nm are incident symmetrically onto a 70 μ m thick LiNbO₃:Fe sample ($c_{Fe} \approx 5.6 \times 10^{19}$ cm⁻³ and $c_{Fe^{2+}}/c_{Fe^{3+}} \approx 0.01$) with a recording angle $2\theta_p = 8^\circ$ outside the crystal. The grating vector is oriented perpendicularly to the crystal's polar axis. The pump pulses are polarized parallel to the polar axis of the crystal and have the same intensity with peak values I_p up to ≈ 170 GW/cm² per pulse inside the sample. The temporal and cross-sectional FWHM of the pump pulse intensity are ≈ 0.22 ps and ≈ 0.7 mm inside the sample. The weak, Bragg-matched probe pulse at $\lambda_r = 776$ nm is displaced by a time Δt by use of a delay stage; it has a FWHM cross section of ≈ 3.5 mm and approximately the same temporal duration as the pump pulse. The optimal overlap of the pulses is obtained by maximizing the detected diffracted pulse energy, and this determines $\Delta t = 0$. Diffraction efficiency η is defined as the energy ratio of the diffracted and transmitted pulses.

Experimental data of $\eta(\Delta t)$ are plotted as circles in Fig. 2. Each circle represents the value of the diffrac-

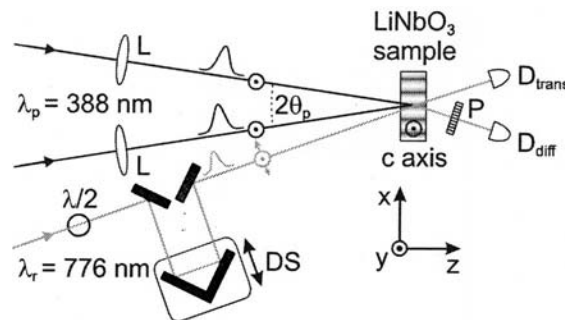


Fig. 1. Schematic illustration of the holographic pump-probe setup in LiNbO₃: λ_p , λ_r , wavelengths of pump and probe pulses, respectively; D, photodiode; DS, delay stage; L, lens; $\lambda/2$, half-wave plate for λ_r ; P, polarizer.

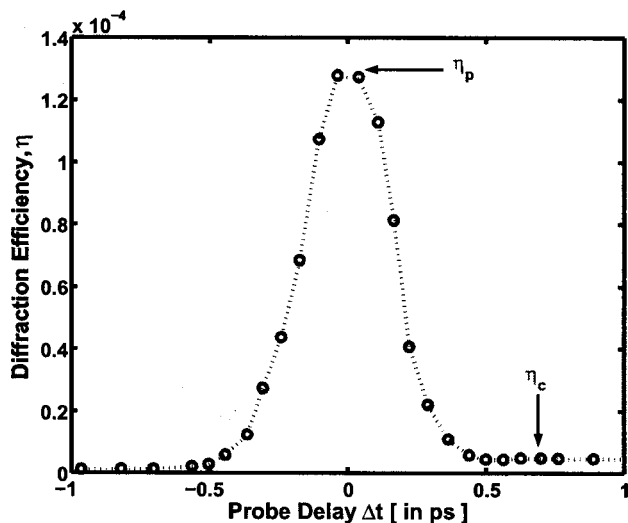


Fig. 2. Diffraction efficiency for $I_p \approx 23 \text{ GW/cm}^2$ and for pump and probe pulses polarized parallel to the crystal polar axis in a $\text{LiNbO}_3:\text{Fe}$ sample with thickness $70 \mu\text{m}$. A theoretical fit yields the Kerr coefficient $n_2 \approx 1.0 \times 10^{-5} \text{ cm}^2/\text{GW}$ for LiNbO_3 . The dotted curve is a guide to the eye.

tion efficiency averaged over 100 single-pulse measurements. After each measurement, uniform illumination is applied to ensure a reproducible starting point for the next measurement. The diffraction efficiency increases rapidly toward a peak value η_p . At $\Delta t \geq 0.5 \text{ ps}$, η remains constant at the value η_c for almost 1 ns; for $\Delta t \geq 1 \text{ ms}$, no diffracted energy can be detected. For a single pair of recording pulses, the energy absorbed is too little to induce any significant photorefractive grating component under our experimental conditions. Doping of the crystals with various amounts of photorefractive impurities does not change the results. Changing the probe light's polarization to be perpendicular to that of the pump pulses gives qualitatively the same curves, with η_p reduced by a factor of ≈ 2.5 .

In general, light diffraction can originate from index and absorption gratings. An instantaneous response can be due to either pump-induced changes in the refractive index because of the Kerr effect or two-color two-photon absorption (involving one pump photon and one probe photon).^{11,12} Longer-lasting effects can arise from charge separation and the electro-optic nonlinearity (photorefractive effect) as well as from index and absorption changes at 776 nm attributed to spatial modulation of the concentration of excited carriers.

From previous studies we know that after the pump pulses come through there is a long-lasting absorption that results from charge carriers excited by two-photon pump absorption (involving two pump photons).¹¹ In our experiment, the photorefractive effect is obviously negligible; otherwise a permanent grating would exist. Furthermore, as the measured η is constant on a picosecond-to-nanosecond time scale, there is also no obvious contribution from a free hot carrier grating.

Based on these facts, we modeled the data shown in Fig. 2, where we have taken into account the dif-

ferent diameters of pump and probe pulses and their spatial and temporal Gaussian shapes as well as the highly nonlinear absorption of the pump pulses. For the longer-lasting effects, the value η_c is explained within the experimental accuracies without any fit parameter by an absorption grating resulting from the spatially modulated carriers that we characterized earlier.^{11,12} The instantaneous response is the combination of the two-color two-photon absorption and the Kerr effect. The two-color two-photon absorption is known from earlier measurements.¹² With Kerr coefficient n_2 as the only fitting parameter, we end up with $n_2 \approx 1.0 \times 10^{-5} \text{ cm}^2/\text{GW}$, which is close to the documented value for 532 nm (Ref. 13) ($\approx 0.83 \times 10^{-5} \text{ cm}^2/\text{GW}$). The index grating from the Kerr effect accounts for $\sim 80\%$ of η_p , and we attribute the other 20% to two-color two-photon absorption. The strong dependence of η_p on the probe polarization confirms that η_p comes predominantly from the Kerr effect, which is known to be strongly dependent on light polarization, while the absorption changes are more-or-less isotropic.¹²

The main reason for the attenuation of the pump light is two-photon pump absorption, and the absorption coefficient is $\beta_p 2I_p$, with $\beta_p \approx 3.5 \text{ cm/GW}$ at 388 nm.¹¹ The values of η_p and η_c are plotted on logarithmic scales as functions of the pump pulse intensity in Fig. 3. The dependence of $\eta_p(I_p)$ is fitted with the function $\eta_p(I_p) \propto I_p^b$, where b is a fit parameter. The data show a turning point of the intensity dependence that lies somewhere near $\beta_p 2I_p d = 1$ (d is the crystal thickness), with $b \approx 1.25$ for $\beta_p 2I_p d > 1$ and $b \approx 2.3$ for $\beta_p 2I_p d < 1$. Dependence $\eta_c(I_p)$ is fitted with the same function, and the extracted exponent b is ≈ 2 .

According to coupled-wave theory of volume grating,¹⁴ diffraction efficiency η depends, for $\eta \ll 1$, quadratically on the product of effective grating thickness L and the grating amplitude, Δn for index gratings and $\Delta\alpha$ for absorption gratings. This is true

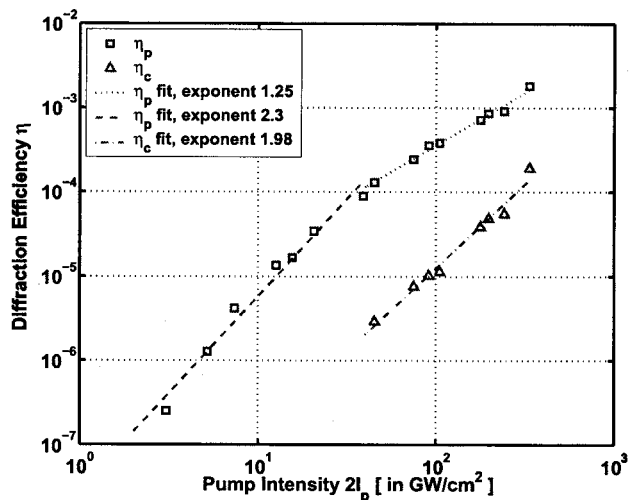


Fig. 3. Summary of measured values of η_p and η_c for different pump intensities I_p in the $70 \mu\text{m}$ $\text{LiNbO}_3:\text{Fe}$ sample. All pulses are polarized along the polar axis of the sample.

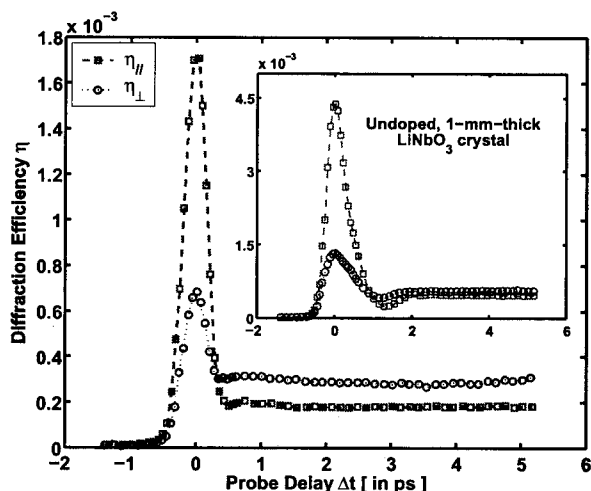


Fig. 4. Diffraction efficiency η as a function of probe delay Δt with peak pump intensities $I_p \approx 170 \text{ GW/cm}^2$ for the $70 \mu\text{m}$ thick crystal. Data acquired from a 1 mm thick, undoped LiNbO_3 sample are plotted in the inset. The pump pulses are polarized along the polar axis, and $\eta_{||}$ (η_{\perp}) is measured when the polarization of the probe pulses is parallel (perpendicular) to that of the pump pulses.

only if Δn and $\Delta\alpha$ are constant throughout the volume of the material. For high pump intensities, strong two-photon pump absorption leads to nonuniform intensity and therefore to nonuniform gratings. Effective interaction length L_{eff} is reduced, and this effect is weaker for the Kerr grating ($\Delta n \propto I_p$) than for the carrier grating ($\Delta\alpha \propto I_p^2$). The experimental results indicate that $L_{\text{eff}} \propto I_p^{-0.5}$ for the Kerr grating and $L_{\text{eff}} \propto I_p^{-1}$ for the carrier grating.

For the low-intensity region $\beta_p 2I_p d < 1$, we have $L_{\text{eff}} \approx d$ for both Kerr and carrier gratings and therefore end up with $\eta_p \propto I_p^2$ and $\eta_c \propto I_p^4$, which is consistent with the experimental observation although in this range η_c is too small to be measured.

In Fig. 4 we show the polarization dependence of the measured diffraction efficiency for $I_p \approx 170 \text{ GW/cm}^2$; the data of $\eta_{||}$ (η_{\perp}) are acquired when the polarization of the probe pulses is parallel (perpendicular) to that of the pump pulses. Plotted in the inset is the result of the same pump-probe experiment carried out in a 1 mm thick undoped LiNbO_3 crystal. As mentioned above, the strong polarization dependence of η_p is a manifestation of the dominant role played by the Kerr grating. All four curves in Fig. 4 show a distinct feature that cannot be observed for low pump intensity (as in Fig. 2): a dip between the descending η and the constant η_c . The reason for the dip of η remains unclear. We point to the possibility of the existence of a transient grating of hot free carriers. The dip can be present because the two

index gratings that are due to the Kerr effect and to the free carriers partially cancel each other. As the lifetime of free carriers inside LiNbO_3 is thought to be smaller than 1 ps, we need even shorter pulses to produce conclusive results. It is worth nothing that, for the highest pump intensities used (in Fig. 4) and for a probe pulse of a reduced diameter (0.7 mm, like that of the pump pulses), diffraction efficiencies of several percent are expected.

We performed pump-probe holographic experiments in LiNbO_3 crystals with femtosecond pulses. Both an instantaneous and a long-lasting grating were observed. We conclusively attribute the instantaneous component to the Kerr effect (contribution, $\approx 80\%$). Furthermore, the excited carriers generate an absorption grating that lasts as long as milliseconds.

We thankfully acknowledge financial support from the National Science Foundation (NSF) Engineering Research Centers Program for Neuromorphic Systems Engineering under award EEC-9402726, from NSF-Germany Cooperative Research grant INT-0233988, from Deutsche Telekom AG, and from the Deutsche Forschungsgemeinschaft (award BU 913/13-1). H.-T. Hsieh's e-mail address is htehsieh@sunoptics.caltech.edu.

References

1. L. Arizmendi, *Phys. Status Solidi A* **201**, 253 (2004).
2. P. Yeh, *Introduction to Photorefractive Nonlinear Optics* (Wiley Interscience, 1993).
3. P. Günter and J. P. Huignard, *Photorefractive Materials and Their Applications* (Springer-Verlag, 1989).
4. P. Boffi, D. Piccinin, and M. C. Ubaldi, *Infrared Holography for Optical Communications* (Springer-Verlag, 2003).
5. J. M. C. Jonathan, G. Roosen, and P. Roussignol, *Opt. Lett.* **13**, 224 (1988).
6. A. L. Smirl, K. M. Bohnert, G. C. Valley, R. A. Mullen, and T. F. Boggess, *J. Opt. Soc. Am. B* **66**, 606 (1989).
7. I. Biaggio, M. Zgonik, and P. Günter, *J. Opt. Soc. Am. B* **9**, 1480 (1992).
8. K. Oba, P. Sun, and Y. Fainman, *Opt. Lett.* **23**, 915 (1998).
9. C. T. Chen, D. M. Kim, and D. von der Linde, *Appl. Phys. Lett.* **34**, 321 (1979).
10. F. Jermann and J. Otten, *J. Opt. Soc. Am. B* **10**, 2085 (1993).
11. O. Beyer, D. Maxein, K. Buse, B. Sturman, H. T. Hsieh, and D. Psaltis, *Opt. Lett.* **30**, 1366 (2005).
12. O. Beyer, D. Maxein, K. Buse, B. Sturman, H. T. Hsieh, and D. Psaltis, *Phys. Rev. E* **71**, 056603 (2005).
13. D. N. Nikogosian, *Properties of Optical and Laser-Related Materials: A Handbook* (Wiley Interscience, 1997).
14. H. Kogelnik, *Bell Syst. Tech. J.* **48**, 2909 (1969).